Acta Cryst. (1984). C**40**, 1–5

The Charge-Density Study of the Laves Phases, $MgZn_2$ and $MgCu_2$

BY T. OHBA, Y. KITANO AND Y. KOMURA

Department of Materials Science, Faculty of Science, Hiroshima University, Higashi-senda-machi, Naka-ku, Hiroshima 730, *Japan*

(*Received* 13 *June* 1983; *accepted* 24 *August* 1983)

Abstract. $MgZn_2$: $M_r = 155{\cdot}05$, hexagonal, $P6_3/mmc$, $a = 5{\cdot}223$ (1), $c = 8{\cdot}566$ (3) Å, $V = 202{\cdot}4$ Å^3, $Z = 4$, $D_x = 5{\cdot}09$ Mg m^{-3}, λ(Mo $K\alpha$) = 0·7107 Å, μ(Mo $K\alpha$) = 24·1 mm^{-1}, $F(000) = 288{\cdot}0$, room temperature. R = 0·0229 for 199 independent reflections. $MgCu_2$: $M_r = 151{\cdot}39$, cubic, $Fd3m$, $a = 7{\cdot}034$ (2) Å, V = 348·0 Å^3, $D_x = 5{\cdot}78$ Mg m^{-3}, $Z = 8$, μ(Mo $K\alpha$) = 25·1 mm^{-1}, $F(000) = 560{\cdot}0$, room temperature. R = 0·0134 for 57 independent reflections. Structure factors for the Laves phases $MgZn_2$ and $MgCu_2$ were measured by X-ray diffraction. The population analysis of valence electrons in $MgZn_2$ and $MgCu_2$ was performed in addition to the refinement of structural parameters using the full-matrix least-squares program. That the kagomé nets in $MgZn_2$ are deformed, in contrast to the case in $MgCu_2$, is analyzed as being due to the different atomic radii for Zn atoms at different positions. Electron transfer from Mg to Zn in $MgZn_2$ and Cu to Mg in $MgCu_2$ was found. Difference Fourier synthesis shows that there are residual electrons at the center of the tetrahedra formed by small atoms, *i.e.* Zn or Cu.

Introduction. Recently, charge-density studies in metals have been performed extensively using the X-ray diffraction method. A charge asphericity in a pure V metal has been found by Ohba, Sato & Saito (1981). They measured integrated intensities of reflection pairs from a spherically shaped single crystal of V metal and discussed the asphericity of the *d*-orbital electrons. Ohba, Saito & Wakoh (1982) have also made a measurement on Cr metal. Bilderback & Colella (1975) measured the 222 forbidden reflection of α-Sn. They analyzed the data using the tetrahedral deformation parameter and found the effect of bonding electrons. Merisalo & Soininen (1979) investigated the bonding electrons in β-Sn with the measurement of the almost-forbidden structure factor of 202 from a flat crystal. The intermetallic compounds V_3Si and Cr_3Si were studied by Staudenmann, Coppens & Muller (1976) and Staudenmann (1977, 1978). They compared the electron density at room temperature with that in the superconducting state.

In the Laves-phase compounds, there are three fundamental structures – $MgZn_2$ ($C14$), $MgCu_2$ ($C15$) and $MgNi_2$ ($C36$) – which were analyzed by Friauf (1927*a*,*b*) and Laves & Witte (1935). These structures are considered as size-factor compounds. The radius ratio ratio r_A/r_B for them is about 1·23. Laves & Witte (1936) and Lieser & Witte (1952) studied the pseudobinary systems of these compounds and found a close relationship between the crystal structure and the electron concentration.

The pseudobinary systems of $MgCu_2$–$MgZn_2$, $MgZn_2$–$MgNi_2$, $MgCu_2$–$MgNi_2$, $MgZn_2$–$MgAg_2$ and $MgCu_2$–$MgAl_2$ were investigated in detail (Komura, 1962; Komura, Mitarai, Nakatani, Iba & Shimizu, 1970; Komura, Nakaue & Mitarai, 1972; Komura, Mitarai, Nakaue & Tsujimoto, 1972; Komura & Kitano, 1977). The authors ascertained that their crystal structures were strongly governed by the electron concentration. In the course of their investigations several stacking variants were found in addition to the three fundamental structures of $C14$, $C15$ and $C36$.

Komura & Tokunaga (1980) have refined the structures of $MgZn_2$, $MgNi_2$, $MgZn_2$–0·03$MgAg_2$($8H$), $MgZn_2$–0·07$MgAg_2$ ($9R$) and $MgZn_2$–0·10$MgAg_2$ ($10H$) using a full-matrix least-squares method.

In order to study the characteristics of the electron-density distribution in the Mg-based Laves phase, we measured the structure factors of single crystals of $MgZn_2$ and $MgCu_2$ accurately and refined the structures by using population analysis and difference Fourier synthesis.

Experimental. Alloy specimens of $MgZn_2$ and $MgCu_2$ were prepared by melting together pure Mg and Zn or Cu in an argon-filled induction furnace. The ingot was crushed into small fragments. A tiny fragment was picked out for the intensity measurement for each compound. The fragment of $MgZn_2$ was shaped into a sphere, but that of $MgCu_2$ was not, since it was nearly spherical. Diameters of the fragments of $MgZn_2$ and $MgCu_2$ were approximately 60 and 40 μm, respectively. Both were confirmed to be single crystals from Laue and oscillation photographs.

Rigaku-automated four-circle diffractometer, graphite monochromator (AFC-5). Monitor counting method used to avoid the effect of the fluctuation of the

0108-2701/84/010001-05$01.50

incident beam. Lattice constants determined by least-squares using 20 reflections ($19° \le 2\theta \le 34°$) for both crystals. Reflections from $MgZn_2$ in a hemisphere of the reciprocal space ($l \ge 0$) out to $2\theta = 70°$ and reflections from $MgCu_2$ in a quarter of the reciprocal space out to $2\theta = 80°$ measured with the θ–2θ scan method, scan rate 2° min^{-1} in θ, scan range $(1{\cdot}5 + 0{\cdot}5 \tan\theta)°$ for $MgZn_2$ and $(1{\cdot}2 + 0{\cdot}5 \tan\theta)°$ for $MgCu_2$. Backgrounds measured at the beginning and end of each scan range. Measurements repeated up to three times until the condition $\sigma(|F_o|)/|F_o| \le 0{\cdot}01$ was satisfied. Four standard reflections measured every 100 reflections; fluctuation of $|F_o|$ of the standard reflections <1·6% for $MgZn_2$, and <3% for $MgCu_2$, so that scaling of reflection data was not made for either crystal. Lp and spherical-absorption corrections applied. Deviations of intensities among equivalent reflections were found to be less than 10%, so the intensities of equivalent reflections with $|F_o| > 3\sigma(|F_o|)$ were averaged to give 199 and 57 independent reflections for $MgZn_2$ and $MgCu_2$, respectively. Full-matrix least-squares refinement on F using *RADIEL* (Coppens, Guru Row, Leung, Stevens, Becker & Yang, 1979); variable parameters: anisotropic temperature factors, an isotropic extinction parameter and populations of the valence electrons for individual atoms in addition to a scale factor and positional parameters. Anomalous-dispersion corrections from *International Tables for X-ray Crystallography* (1974). When the ordinary atomic scattering factors in *International Tables for X-ray Crystallography* (1974) were used, the reliability factors $R_w(F)$ were 1·44% for $MgZn_2$ and 1·20% for $MgCu_2$. The population analysis was next performed using Fukamachi's (1971) atomic scattering factors. The core electrons of Mg were assumed to be those of Ne, and the core electrons of Zn and Cu to be those of Ar. Valence electrons were assumed to be $(3s)^2$, $(3d)^{10}(4s)^2$ and $(3d)^{10}(4s)^1$ for Mg, Zn and Cu, respectively. The total charge was kept constant in the refinements by application of a neutrality constraint. By the population analysis, $R_w(F)$ values reduced to 1·39% and 1·17% for $MgZn_2$ and $MgCu_2$, respectively.* The largest correlation coefficients between the scale factor and population parameter were 0·75 for $MgZn_2$ and 0·66 for $MgCu_2$. $w = 1/\sigma_F^2$, $(\Delta/\sigma)_{max} = 0{\cdot}1$, final $\Delta\rho$ excursions $\le |2{\cdot}0|$ e $Å^{-3}$.

Discussion. The final parameters obtained are shown in Table 1. The positional parameters of $MgZn_2$ are in agreement with those reported by Komura & Tokunaga (1980) within the standard deviations, although anisotropic instead of isotropic temperature factors were used in the present analysis. The structure of $MgCu_2$ has been refined for the first time.

The cubic $MgCu_2$ structure can be described in terms of a hexagonal axis, if [111] of the cubic unit cell is taken as the c axis of the hexagonal cell. Then the kagomé net on the (001) plane is formed by the regular triangles and hexagons as shown in Fig. 1(*a*), the Cu atoms being placed at each cross point. Cu atoms placed off the kagomé net are also shown by circles. The kagomé net in $MgZn_2$ is shown in Fig. 1(*b*); Zn atoms placed above and below the net are included in the figure. Table 1 shows that Zn(2) in $MgZn_2$ is shifted from the position which would form regular triangles and hexagons in the kagomé net. The directions of atom shifts are also shown by arrows in Fig. 1(*b*). As a result the kagomé net is formed by two kinds of triangles and hexagons. One of the triangles is larger than the other, and the hexagons are no longer regular. The larger triangles in $MgZn_2$ form tetrahedra with Zn(1) atoms which are shown by filled circles.

The shape of the thermal ellipsoid of Mg in $MgZn_2$ is almost a sphere, whereas the length along the c axis of the ellipsoid of Zn(1) is 20% shorter than that in the ab plane. The axis of the ellipsoid of Zn(2) along the direction in which the atom is shifted is 20% shorter

* Lists of structure factors for $MgZn_2$ and $MgCu_2$ have been deposited with the British Library Lending Division as Supplementary Publication No. SUP 38860 (4 pp.). Copies may be obtained through The Executive Secretary, International Union of Crystallography, 5 Abbey Square, Chester CH1 2HU, England.

Table 1. *Refined parameters for* $MgZn_2$ *and* $MgCu_2$

'Valence' in the table represents an increase (+) or a decrease (–) of the valence electrons from the neutral atoms. g is an extinction parameter. T.F. $= \exp(-2\pi^2 \sum_i \sum_j U_{ij} h_i h_j a_i^* a_j^*)$.

$MgZn_2$

		Valence	x	y	z	U_{11}	U_{22}	U_{33}	U_{12}	U_{13}	U_{23}
Mg	4(*f*)	−0·559 (180)	$\frac{1}{3}$	$\frac{2}{3}$	0·06286 (13)	0·01328 (34)	U_{11}	0·01386 (50)	$U_{11}/2$	0·0	0·0
Zn(1)	2(*a*)	+0·396 (108)	0·0	0·0	0·0	0·01427 (17)	U_{11}	0·00809 (21)	$U_{11}/2$	0·0	0·0
Zn(2)	6(*h*)	+0·236 (92)	−0·16952 (4)	$2x$	0·25	0·01311 (13)	0·00844 (15)	0·01352 (12)	$U_{22}/2$	0·0	0·0
		$g = 0{\cdot}1467\ (70) \times 10^{-4}$									

$MgCu_2$

		Valence	x	y	z	U_{11}	U_{22}	U_{33}	U_{12}	U_{13}	U_{23}
Mg	8(*a*)	+0·576 (244)	$\frac{1}{8}$	$\frac{1}{8}$	$\frac{1}{8}$	0·01087 (43)	U_{11}	U_{11}	0·0	0·0	0·0
Cu	16(*d*)	−0·288 (124)	$\frac{1}{2}$	$\frac{1}{2}$	$\frac{1}{2}$	0·01043 (15)	U_{11}	U_{11}	−0·00144 (10)	U_{12}	U_{12}
		$g = 0{\cdot}104\ (13) \times 10^{-4}$									

than the other principal axes. The thermal ellipsoid of Cu in $MgCu_2$ is almost a sphere.

Table 1 shows that in $MgZn_2$ the electron transfer takes place from Mg to Zn. This is consistent with the calculation performed by Rennert & Radwan (1977). They investigated the stability of the structure of $MgZn_2$ using Shaw's model potential and showed that the charge transfer from Mg to Zn plays an important role. Hafner (1979) calculated the charge-density distribution in CsK_2 which has a $MgZn_2$-type structure. He reported that in CsK_2 the electronic charge around Cs is less than that of pure Cs ion-core and the charge around K is more than that of pure K ion-core and a few residual electrons are found in an interstitial region. Although the elements are different, the direction of the charge transfer is the same as in $MgZn_2$. Haydock & Johannes (1975) calculated the electronic structure of a transition-metal Laves phase. However, they did not consider the effect of the charge transfer or of the charge-density distribution in the real space. On the other hand, Table 1 reveals that the electrons in Cu in $MgCu_2$ move to Mg. The direction of the electron transfer of $MgCu_2$ is opposite to that of $MgZn_2$.

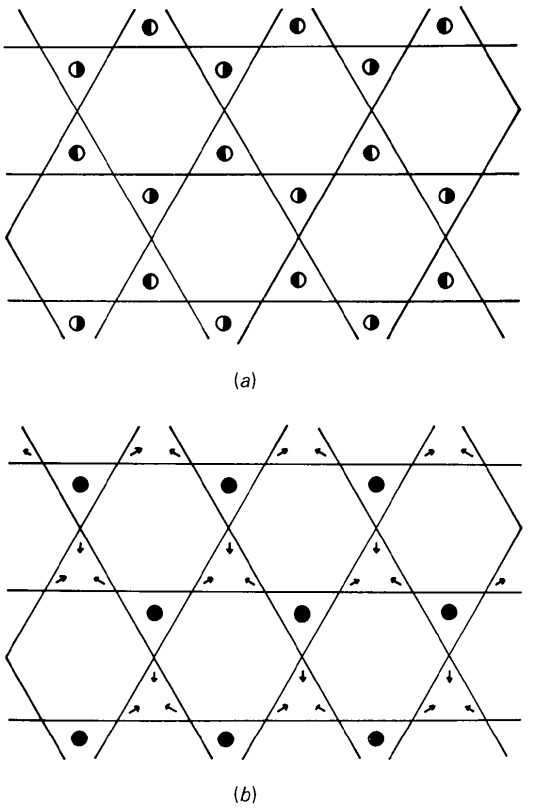

(*a*)

(*b*)

Fig. 1. (*a*) Kagomé net in $MgCu_2$. (*b*) Kagomé net in $MgZn_2$. Atoms Cu or Zn are placed at every cross point of the lines. ◑ atoms placed below the net; ◐ atoms above the net; ● atoms placed above and below the kagomé net. Arrows indicate the directions of atom shifts.

Table 2. *Interatomic distances* (Å) *for* $MgZn_2$ *and* $MgCu_2$

$MgZn_2$			$MgCu_2$		
Mg			Mg		
Mg	(×1)	3·2061 (20) Å	Mg	(×4)	3·0458 (5) Å
Mg	(×3)	3·2021 (5)	Cu	(×12)	2·9161 (7)
Zn(1)	(×3)	3·0632 (6)	Cu		
Zn(2)	(×3)	3·0624 (13)	Mg	(×6)	2·9161 (7)
Zn(2)	(×6)	3·0644 (6)	Cu	(×6)	2·4869 (5)
Zn(1)					
Mg	(×6)	3·0632 (6)			
Zn(2)	(×6)	2·6340 (7)			
Zn(2)					
Mg	(×2)	3·0624 (13)			
Mg	(×4)	3·0644 (8)			
Zn(1)	(×2)	2·6340 (7)			
Zn(2)	(×2)	2·6562 (5)			
Zn(2)	(×2)	2·5668 (8)			

The interatomic distances in $MgZn_2$ and $MgCu_2$ are shown in Table 2. Those in $MgZn_2$ are almost the same as those given in a previous paper (Komura & Tokunaga, 1980). On the basis of the spherical-atom model, we can understand that if the atomic radii of Zn(1) and Zn(2) were the same as those of Cu in $MgCu_2$, the kagomé net would not be deformed. The fact that the kagomé net is deformed suggests that the atomic radii of Zn(1) are different from those of Zn(2). Table 1 shows that the Zn(1) atoms have more electrons than the Zn(2) atoms; therefore, it can be assumed the atomic radii of Zn(1) are larger than those of Zn(2). The larger atoms Zn(1) repel the sandwiched atoms Zn(2) which form the triangles in the kagomé net as seen in Fig. 1(*b*).

Interatomic distances in Table 2 show that those between Zn(1) and Zn(2) are larger than the average distance 2·6115 (5) Å between Zn(2) and Zn(2). In a previous paper, Komura & Tokunaga (1980) reported that, in $MgNi_2$ and other long-period structures, the kagomé nets which are in the mode of connection of the $MgZn_2$ structure are also deformed, whereas those in the mode of connection of the $MgCu_2$ structure are not deformed. Therefore, the deformation of the kagomé net may probably be caused by the difference in the atomic radii mentioned above.

Difference Fourier maps of $MgZn_2$ synthesized with the coefficients (F_o-F_c) after the population analysis are shown in Fig. 2. They are shown in sections every $c/16$ parallel to (001). In this figure, there are residual electrons at the corner of the unit cell on the section $z=\frac{3}{16}$. Their positions are at the centers of the tetrahedra formed by Zn atoms. Above the Mg atom on the plane $z=\frac{1}{16}$, there are also residual electrons at $z=\frac{2}{16}$. The section at $z=\frac{4}{16}$ shows the steepest hills and valleys; this may be related to the fact that the Zn(2) atoms on this plane are shifted from the positions which form the regular hexagons. The difference Fourier section through the kagomé net in the cubic $MgCu_2$ corresponding to the plane $z=\frac{4}{16}$ in Fig. 2 is shown in Fig. 3(*a*). The map shows a smoother feature than that

of $MgZn_2$. In Fig. 3(*b*) the section parallel to (001) of $MgCu_2$ is shown. The positions $\frac{1}{8}$, $\frac{5}{8}$, $\frac{1}{8}$ and $\frac{5}{8}$, $\frac{1}{8}$, $\frac{1}{8}$ on the plane $z=\frac{1}{8}$ are the centers of the tetrahedra formed by Cu atoms at $z=0$ and $z=\frac{1}{4}$. Residual electrons are found at these positions just as in the case of $MgZn_2$ in Fig. 2. Although the directions of charge transfer are opposite, the residual electrons in both $MgZn_2$ and $MgCu_2$ are found at the centers of the tetrahedra formed by small atoms. In the Laves-phase structure, there are many kinds of tetrahedra formed by large (A) and small (B) atoms; that is, AB_3, A_2B_2 and B_4 aggregate for the AB_2-type Laves phase. The residual electrons, however, are not found at the centers of tetrahedra except for B_4 tetrahedra formed by major small component atoms. Edward (1972) noted a qualitative relationship between the structure of the element of major small atoms and the occurrence of $C14$ or $C15$ in the Laves phase. In the present study, the residual electrons are found at the centers of the tetrahedra which are formed by major small atoms.

There are two kinds of coordination polyhedra in the Laves phase: CN12 icosahedron and CN16 Friauf polyhedron (Samson, 1958). There are no bonding electrons between the central atom and surrounding atoms in these polyhedra from inspection of difference Fourier maps. Charge asphericity around the atoms is observed in some cases; for example, there are residual electrons above the Mg atoms in $MgZn_2$ ($z=\frac{2}{16}$). However, a detailed analysis of the asphericity seems to be difficult with the present data.

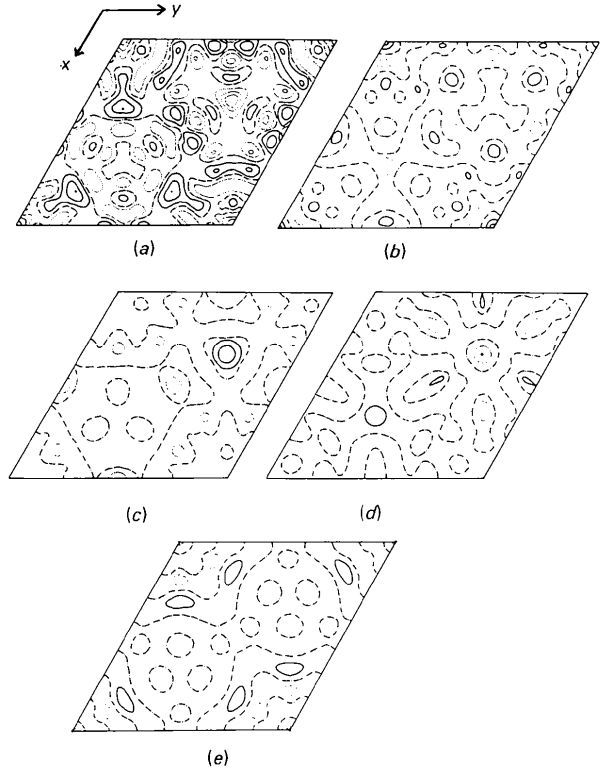

Fig. 2. Difference Fourier maps of $MgZn_2$, sections parallel to the (001) plane. The contour interval is $0{\cdot}5$ e Å^{-3} and solid and dotted lines represent positive and negative contours, respectively. Zn atoms are placed on the planes $z=0$ and $z=\frac{1}{4}$ and are indicated by black dots. (*a*) $z=\frac{4}{16}$, (*b*) $z=\frac{3}{16}$, (*c*) $z=\frac{2}{16}$, (*d*) $z=\frac{1}{16}$, (*e*) $z=0$.

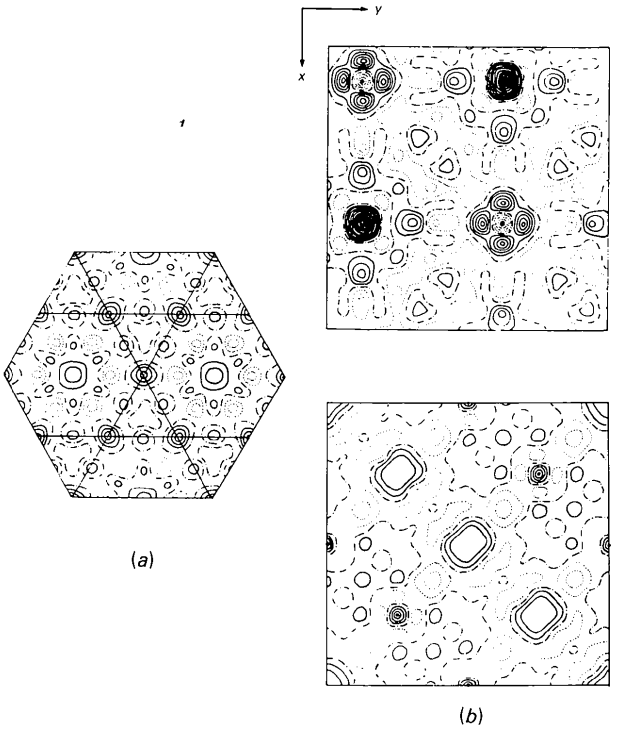

Fig. 3. Difference Fourier maps of $MgCu_2$. (*a*) (111) plane. Cu atoms are placed at every cross point of the lines and form the kagomé net. (*b*) Sections parallel to the (001) plane (upper, $z=\frac{1}{8}$; lower, $z=0$). The contour interval is $0{\cdot}1$ e Å^{-3} and solid and dotted lines represent positive and negative contours, respectively. On the plane $z=0$, small atoms Cu are placed at $\frac{1}{2}$,0,0; $\frac{1}{4}$,$\frac{3}{4}$,0; 0,$\frac{1}{2}$,0 and $\frac{3}{4}$,$\frac{1}{4}$,0 as indicated by black dots.

We wish to thank Professor P. Coppens of the State University of New York at Buffalo for allowing us to use the program *RADIEL* and Professor Y. Saito and Dr S. Ohba of Keio University for valuable advice in using the program. The calculations were carried out on HITAC M-180 and M-200H computers at the Information Processing Center of Hiroshima University. The present work has partly been supported by a Scientific Research Grant from the Ministry of Education, Science and Culture to which authors' thanks are due.

References

BILDERBACK, D. H. & COLELLA, R. (1975). *Phys. Rev. B*, **11**, 793–797.

COPPENS, P., GURU ROW, T. N., LEUNG, P., STEVENS, E. D., BECKER, P. & YANG, Y. W. (1979). *Acta Cryst.* A**35**, 63–72.
EDWARD, A. R. (1972). *Metall. Trans.* **3**, 1365–1372.
FRIAUF, J. B. (1927*a*). *Phys. Rev.* **29**, 35–40.
FRIAUF, J. B. (1927*b*). *J. Am. Chem. Soc.* **49**, 3107–3114.
FUKAMACHI, T. (1971). *Tech. Rep. Inst. Solid State Phys. Tokyo Univ.* B12.
HAFNER, J. (1979). *Phys. Rev. B*, **19**, 5094–5102.
HAYDOCK, R. & JOHANNES, R. L. (1975). *J. Phys. F*, **5**, 2055–2067.
International Tables for X-ray Crystallography (1974). Vol. IV. Birmingham: Kynoch Press.
KOMURA, Y. (1962). *Acta Cryst.* **15**, 770–778.
KOMURA, Y. & KITANO, Y. (1977). *Acta Cryst.* B**33**, 2496–2501.
KOMURA, Y., MITARAI, M., NAKATANI, I., IBA, H. & SHIMIZU, T. (1970). *Acta Cryst.* B**26**, 666–668.
KOMURA, Y., MITARAI, M., NAKAUE, A. & TSUJIMOTO, S. (1972). *Acta Cryst.* B**28**, 976–978.
KOMURA, Y., NAKAUE, A. & MITARAI, M. (1972). *Acta Cryst.* B**28**, 727–732.
KOMURA, Y. & TOKUNAGA, K. (1980). *Acta Cryst.* B**36**, 1548–1554.
LAVES, F. & WITTE, H. (1935). *Metallwirtsch. Metallwiss. Metalltech.* **14**, 645–649.
LAVES, F. & WITTE, H. (1936). *Metallwirtsch. Metallwiss. Metalltech.* **15**, 840–842.
LIESER, K. H. & WITTE, H. (1952). *Z. Metallkd.* **43**, 396–401.
MERISALO, M. & SOININEN, J. (1979). *Phys. Rev. B*, **19**, 6289–6294.
OHBA, S., SAITO, Y. & WAKOH, S. (1982). *Acta Cryst.* A**38**, 103–108.
OHBA, S., SATO, S. & SAITO, Y. (1981). *Acta Cryst.* A**37**, 697–701.
RENNERT, P. & RADWAN, A. M. (1977). *Phys. Status Solidi B*, **79**, 167–173.
SAMSON, S. (1958). *Acta Cryst.* **11**, 851–857.
STAUDENMANN, J. L. (1977). *Solid State Commun.* **23**, 121–125.
STAUDENMANN, J. L. (1978). *Solid State Commun.* **26**, 461–468.
STAUDENMANN, J. L., COPPENS, P. & MULLER, J. (1976). *Solid State Commun.* **19**, 29–33.

Acta Cryst. (1984). C**40**, 5–7

The Structure of Hexapotassium Disodium Hexatungstoplatinate(IV) Dodecahydrate, $K_6Na_2[PtW_6O_{24}].12H_2O$

BY UK LEE,* HIKARU ICHIDA, AKIKO KOBAYASHI AND YUKIYOSHI SASAKI

Department of Chemistry and Research Centre for Spectrochemistry, Faculty of Science, The University of Tokyo, Hongo, Tokyo 113, *Japan*

(*Received* 11 *April* 1983; *accepted* 24 *August* 1983)

Abstract. $M_r = 2178{\cdot}77$, trigonal, $R\bar{3}m$, $a = 9{\cdot}740$ (1) Å, $\alpha = 84{\cdot}81$ (1)°, $U = 913{\cdot}3$ (1) Å^3, $Z = 1$, $D_x = 3{\cdot}961$ g cm^{-3}, Mo $K\alpha$ radiation ($\lambda = 0{\cdot}7107$ Å), μ(Mo $K\alpha$) = 247·3 cm^{-1}, $F(000) = 970$, $T = 298$ K. The structure was determined by the heavy-atom method and refined by the block-diagonal least-squares method. The final $R = 0{\cdot}059$ for 859 independent reflections collected by diffractometry. The heteropolyanion has a structure with point symmetry D_{3d} ($\bar{3}m$) of the ideal Anderson-type heteropolyanion. The Pt—W and W—W distances are 3·238 (1) Å. Three types of W—O (W—O_t, W—O_b and W—O_c) distances are 1·75 (1), 1·97 (2) and 2·16 (2) Å.

Introduction. Recently we reported the synthesis and crystal structure of $Na_5[H_3PtW_6O_{24}].20H_2O$ (Lee, Kobayashi & Sasaki, 1983). Some heteropolytungstates containing platinum have been reported by Gibbs (Pt:W = 1:10, 1:20, 2:30 and 1:30) and Rosenheim (Pt:W = 2:7) (*Gmelin's Handbuch der Anorganischen Chemie*, 1933), but their syntheses could not be reproduced in our laboratory. We report here the structure of the unprotonated heteropolyanion $[PtW_6O_{24}]^{8-}$ obtained at pH *ca* 7·5.

Experimental. 0·81 g of $K_2WO_4.2H_2O$ was dissolved in 40 ml of hot water. To this solution 40 ml of 0·16 g $K_2Pt(OH)_6$ solution (containing a small portion of Na^+ ion) was added dropwise and 3*M* HNO_3 was used to adjust the pH to *ca* 6·0. After the mixture was heated for half an hour on the water bath and cooled, the pH was adjusted to *ca* 7·5. Small pale-yellow hexagonal crystals were obtained after two days when the solution was concentrated to about 70 ml at room temperature. The crystals are stable in air and a TGA–DSC diagram showed that the water molecules (0·95 w%) were slowly lost from the crystals in the temperature range 356–411 K.

A single crystal of dimensions 0·13 × 0·14 × 0·08 mm, Rigaku automated four-circle diffractometer, graphite monochromator, cell parameters refined by least-squares method on the basis of 25 independent indices ($40 < 2\theta < 45°$), Mo $K\alpha$ radiation ($\lambda = 0{\cdot}7107$ Å); intensity measurement performed to $2\theta = 60°$ (the $+h$, $+k$, $+l$ set), ω–2θ scan method, scan

* Permanent address: Department of Chemistry, College of Natural Science, Busan National University, Busan 607, Korea.

0108-2701/84/010005-03$01.50